

Defect Microchemistry at the SiO₂/Si Interface

G. W. Rubloff, K. Hofmann,^(a) M. Liehr, and D. R. Young^(b)

IBM Thomas J. Watson Research Center, Yorktown Heights, New York 10598

(Received 21 November 1986)

The intrinsic oxide decomposition reaction $\text{Si} + \text{SiO}_2 \rightarrow 2\text{SiO} \uparrow$ at the SiO₂/Si interface is shown to be nucleated at existing defect sites prior to the growth of physical oxide voids. At lower temperatures than needed for void formation, these defects become electrically active, leading to low-field dielectric breakdown unless sufficient O₂ is available (low concentrations). The systematics of the required O₂ suggests strongly that it reverses the initial decomposition by reoxidizing the SiO product at the interface.

PACS numbers: 82.30.Lp, 64.80.Gd, 68.35.-p

Thermal oxidation of Si yields thin SiO₂ layers of extremely high dielectric quality which form the basis for Si field-effect-transistor (FET) technology. Research has yielded significant advances in characterizing defects in such systems from a fundamental¹ point of view. Our ability to minimize and/or control such defects plays a crucial role in the advance of the technology: For example, chemical treatment of defects by postoxidation ambient annealing processes is a prerequisite for producing state-of-the-art FET gate oxides. Although the correlation of ambient annealing processes with oxide electrical quality suggests models for the underlying defect chemistry, the *microscopic chemistry of defects* in Si/SiO₂ systems is little understood.

Recent work has begun to elucidate the microscopic chemistry of typical bonding arrangements in these systems,² including those of high-density defects ($\sim 10^{13}$ – 10^{15} cm⁻²) which can be observed by use of surface-analysis techniques. While these results carry significant insight, it remains a challenge to define how they relate to the lower-density defects which dominate electrical properties, such as charge trapping states ($\sim 10^{10}$ cm⁻²) or dielectric-breakdown sites ($\sim 10^3$ cm⁻²) in high-quality structures.

The microscopic chemistry of the oxide decomposition reaction $\text{Si} + \text{SiO}_2 \rightarrow 2\text{SiO} \uparrow$ has recently been shown³ to involve lateral consumption of the oxide: Voids are formed entirely through the oxide to expose the Si surface, and the voids grow in diameter by surface self-diffusion of Si atoms to the oxide at the periphery of the void. The lateral inhomogeneity of the reaction suggests the possibility that defects play a role in the process,³ and initial measurements of void density and size distribution during the reaction are consistent with a picture of defects as the nucleation site for the reaction.^{4,5}

We report here the detailed kinetics of oxide-void growth induced by vacuum annealing, which demonstrates clearly that oxide decomposition reaction is initiated at defect sites already present in the Si/SiO₂ structure and thus provides an effective means for decorating microscopic defects. Annealing at ~ 750 – 900°C (insufficient for void growth) transforms these defects

into an electrically active state which causes low-field dielectric breakdown. Both observations are consistent with enhanced oxide decomposition ($\text{Si} + \text{SiO}_2 \rightarrow 2\text{SiO}$) at the defect site. With sufficient O₂ (ppm level) present during annealing, low-field breakdown is prevented, providing a means for chemical control of defects; the temperature dependence of the O₂ concentration needed implies that the O₂ acts to reoxidize the SiO product at the defect.

Dry thermal SiO₂ layers 500 Å thick of device quality were grown on Si(100) at 900–1000°C. Postoxidation annealing at 750–1175°C was carried out in ultrahigh vacuum,³ in some cases with low partial pressures of O₂ purposely present. A scanning Auger microscope was used to obtain both scanning-Auger-microscopy and scanning-electron-microscopy (SEM) images for the void kinetics studies.⁵ For the electrical measurements, metal-oxide-semiconductor (MOS) capacitors were then formed by evaporation of 2000-Å-thick Al dots (0.032-in. diam) through a mask, by use of an rf-heated crucible. Ramped dark current-voltage (*I-V*) measurements with positive gate bias were employed to characterize low-field breakdown.⁶

From SEM micrographs of the Si/SiO₂ surface, it has been possible to determine the oxide-void density and size distribution at various stages of annealing. An example of this is shown in Fig. 1 for annealing at 1175°C, which represents a lateral range of observation of 0.3×0.7 mm² and a void density $\sim 10^2$ mm⁻². After an incubation time required to generate voids of sufficient size to be observable, the number of voids present does not increase significantly with time. In addition, the size distribution for most voids remains quite sharp (narrow) as the voids grow in diameter. Both observations demonstrate that a few new voids are formed spontaneously under annealing conditions; rather, the voids must be characteristic of sites (defects) which were already present in the structure before the annealing began. This is extremely strong evidence that the void growth process is nucleated at existing defect sites and thus provides a method for decorating (revealing) microscopic defects.

It is also evident from Fig. 1 that a considerably small-

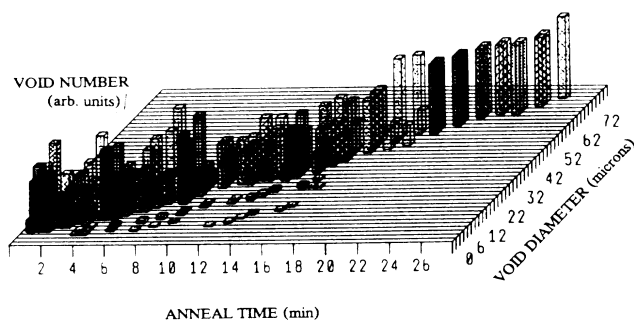


FIG. 1. Size distribution of oxide voids obtained by absorbed current SEM micrographs for a dry thermal oxide annealed in vacuum at 1175°C. Voids were observed over an area $0.3 \times 0.7 \text{ mm}^2$ at density $\sim 10^2 \text{ mm}^{-2}$.

er number of additional voids are formed somewhat later in time. These "minority species" of voids grow at what appears to be the same rate as the majority species of voids, suggesting that the lateral growth of the void after nucleation is independent of the nature of the nucleating defect. It may well be that the nucleation times of different types of defects differ, thus distinguishing different defects by their different sizes at a given stage of annealing. Nevertheless, the sample represented in Fig. 1 contained mainly one species of defect. We may expect the size distribution of voids to be much broader and/or complicated if several defect types were to be present in comparable numbers. Additional defects associated with metal impurities⁷ or preoxidation implantation damage⁸ produce larger numbers of additional voids.

It is important to note that the defect sites which nucleate the decomposition reaction to form physical voids in the oxide are normally not electrically active: MOS capacitors fabricated from oxides like those studied here show excellent electrical characteristics, e.g., $\geq 8\text{--}9\text{-MV/cm}$ breakdown fields without low-field breakdown events. However, one would expect some electrical manifestation of the evolution/growth of the initial defect before it becomes a physical void in the oxide as a result of annealing. Annealing in sufficiently oxygen-deficient conditions (either vacuum or clean inert gas) indeed reveals the activation of electrical defects for temperatures $\geq 750^\circ\text{C}$.

As an example, Fig. 2 shows the I - V characteristics for MOS capacitors produced after 900°C vacuum annealing with different O_2 partial pressures present. Without postoxidation annealing (POA), the current remains low and constant until Fowler-Nordheim (field-assisted) tunneling begins near 6 MV/cm. However, with annealing at low O_2 pressures of 5×10^{-6} or 5×10^{-3} Torr, low-field breakdown (LFB) events occur as indicated by excessive current levels at fields $< 6 \text{ MV/cm}$. (Vacuum annealing, not shown here, is very similar to the

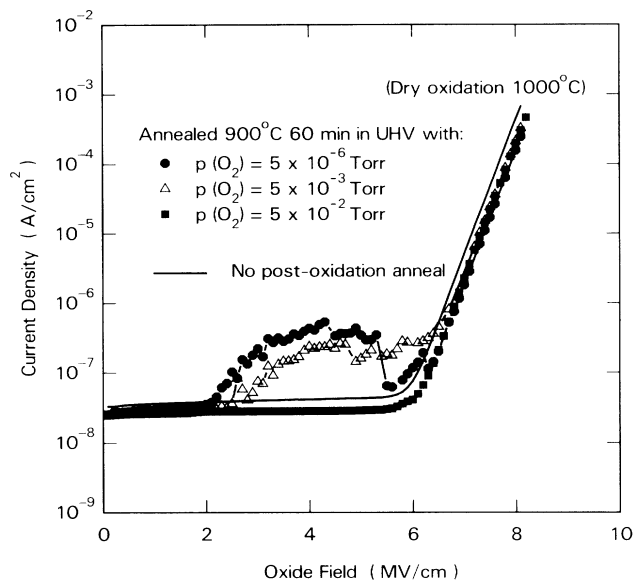


FIG. 2. Typical ramped I - V curves for MOS structures annealed at 900°C in O_2 ambients of various pressures.

5×10^{-6} -Torr result.) These LFB events are indicative of a deleterious defect in the MOSA structure, which renders it useless for a device.

In contrast, if a sufficiently large concentration of O_2 is present in the annealing ambient, low-field breakdown does not occur. This is demonstrated by the characteristic for 5×10^{-2} Torr O_2 in Fig. 2. Note that in this case a characteristic essentially identical to that of the control (no POA) is obtained. Thus the presence of *sufficient* oxygen during annealing prevents the formation of the *electrical* defect. It is natural to assume that the electrical defects shown here evolve from the same microscopic defect (originally inactive electrically) which nucleates the decomposition reaction and leads to the formation of oxide voids.

From such measurements we have established the systematics of the O_2 concentration required to prevent low-field breakdown. In the form of an Arrhenius plot, Fig. 3 shows as squares the various combinations of O_2 partial pressure and annealing temperature (during POA) for which we determined the presence or absence of LFB events. Solid symbols indicate that no LFB was observed, open symbols the opposite. Note that the parameter space for the prevention of LFB is rather sharply separated from that where LFB occurs, as represented by the line p_{crit} . Ultrahigh-vacuum annealing also yields LFB. Thus a minimum O_2 partial pressure is required at a given temperature to prevent LFB. Furthermore, results are also shown in Fig. 3 for annealing in low partial pressures of N_2 and Ar. Since pressures above p_{crit} do not prevent LFB, we conclude that O_2 , not N_2 or Ar, is required. (Other oxygen-containing species like H_2O

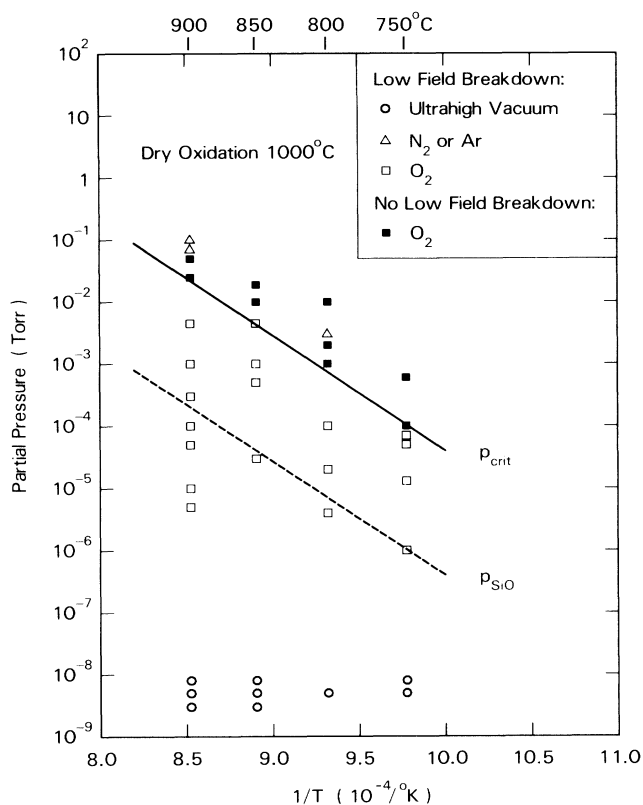


FIG. 3. Effect of O_2 pressure on low-field breakdown in SiO_2 films (500 Å) annealed for 60 min at 750 to 900°C. Solid and open symbols represent annealing conditions without and with breakdown degradation, respectively. The critical O_2 pressure for suppression of low-field breakdown is indicated by the solid line. Also shown is the equilibrium pressure for SiO (dashed line).

might also suffice, a possibility yet to be explored.)

Figure 3 also shows as the line labeled p_{SiO} the temperature-dependent vapor pressure of SiO , the product of the decomposition reaction. It is significant that the "phase boundary" p_{crit} has the same slope (activation energy) as the slope of SiO desorption. This reveals that electrical defects leading to LFB are prevented by the supplying of O_2 faster than the release of SiO , assuming this to be the rate-limiting step in transforming defects into an electrically active state (for LFB). This suggests that the O_2 acts to reoxidize the SiO product to a non-deleterious state (e.g., SiO_2) by the reaction $2SiO + O_2 \rightarrow 2SiO_2$. To provide an O_2 pressure at the interface (where the reaction begins) sufficient to balance the SiO vapor pressure may require a higher O_2 pressure over the oxide surface; this may explain the vertical displacement of the p_{crit} from the p_{SiO} lines in Fig. 3.

The results in Fig. 3 demonstrate clearly that low concentrations of O_2 are required during annealing in order

to prevent low-field breakdown. In principle, this provides a method for defect control, since it is unlikely that technology would ever be able to prevent defects entirely. In view of these results, it might be surprising that high-quality FET oxides are *ever* produced, because inert-gas ambient annealing in these temperature ranges are routine steps to device fabrication. The answer lies in the actual concentrations needed: E.g., in a typical 1-atm POA furnace, the 10^{-4} Torr O_2 needed at 750°C would correspond to ~ 0.1 ppm. Such pure furnace environments are extremely difficult to achieve, and LFB problems as described here should be expected only in some future generation of processing equipment.

Together with previous results concerning the microscopic chemistry of oxide decomposition in Si/SiO_2 structures,³ one obtains a picture of three stages of defect evolution. Initially a microscopic defect which exists may well be inactive with respect to some electrical characteristic (e.g., LFB). With annealing, the decomposition reaction which dominates oxide-void growth also occurs preferentially at that defect site in order to nucleate the formation of the oxide void. It is not surprising that the activation energy is somewhat lowered at a defect site (cf. an ideal bonding site), since the local chemical bonding there is certainly disturbed from the ideal in some way.

During the evolution of the defect by annealing, the defect becomes electrically active, e.g., as in low-field breakdown. At a later stage the reaction around the defect proceeds far enough to produce a microvoid sufficient to permit escape of the SiO decomposition product. If an additional reactant (O_2) is supplied at sufficient rate to the defect, the chemistry may be driven toward stability of the structure by the reoxidizing of the SiO decomposition product to SiO_2 , thus reforming the interface which was degraded by the decomposition reaction.

In this work we have studied the microchemistry of defects associated with low-field breakdown, which occur at very low density (perhaps $\sim 10^3$ cm^{-2}). We have also found⁹ that hole-trapping rates increase under similar oxygen-deficient conditions but decrease with sufficient O_2 concentrations during annealing. Since such trapping states occur at higher density (perhaps $\sim 10^{10}$ cm^{-2}), related versions of this defect microchemistry may affect other kinds of defect bonds in Si/SiO_2 structures than those which dominate breakdown. Further studies of other gaseous species and toward the range of higher total pressures are planned. This work underscores the potential of research which couples a high degree of control of chemical processes to the electrical figures of merit for the thin film and/or interface of interest.

We are grateful to M. Bradley and S. I. Raider for valuable discussions. We thank J. E. Lewis for cooperation in the SEM studies and J. Calise for growing the ox-

ides and depositing the Al contacts. This work is sponsored in part by the U.S. Office of Naval Research.

^(a)Permanent address: Forschungsinstitut, Allgemeine Elektrizität-Gesellschaft Telefunken, D-7900 Ulm, Federal Republic of Germany.

^(b)Permanent address: Fairchild Laboratory, Lehigh University, Bethlehem, PA 18015.

¹G. J. Geradi, E. H. Poindexter, P. J. Caplan, and N. M. Johnson, *Appl. Phys. Lett.* **49**, 348 (1986); P. J. Caplan, E. H. Poindexter, B. E. Deal, and R. R. Razouk, *J. Appl. Phys.* **50**, 5847 (1979).

²G. Hollinger and F. J. Himpsel, *Appl. Phys. Lett.* **44**, 93 (1984); M. Sobolewski and C. R. Helms, *J. Vac. Sci. Technol. A* **3**, 1300 (1985); F. J. Grunthaner, B. F. Lewis, J. Maserjian,

and A. Madhukar, *J. Vac. Sci. Technol.* **20**, 747 (1982).

³R. Tromp, G. W. Rubloff, P. Balk, F. K. LeGoues, and E. J. van Loenen, *Phys. Rev. Lett.* **55**, 2332 (1985).

⁴K. Hofmann, G. W. Rubloff, and R. A. McCorkle, *Appl. Phys. Lett.* (to be published).

⁵M. Liehr, J. E. Lewis, and G. W. Rubloff, *J. Vac. Sci. Technol. A* (to be published).

⁶K. Hofmann, G. W. Rubloff, and D. R. Young, to be published.

⁷M. Kobayashi, T. Ogawa, and K. Wada, in *Extended Abstracts of The Electrochemical Society, Canada, 1985* (Electrochemical Society, Pennington, NJ, 1985), Vol. 85-I, No. 66, p. 94.

⁸S. I. Raider, K. Hofmann, and G. W. Rubloff, to be published.

⁹K. Hofmann, D. R. Young, and G. W. Rubloff, to be published.